Effects of manufacturing errors on the characteristics of a polymer vertical coupling microring resonator*

Wang Yuhai(汪玉海), Qin Zhengkun(秦政坤)†, Wang Chunxu(王春旭), and Wang Lizhong(王立忠)

College of Information and Technology, Jilin Normal University, Siping 136000, China

Abstract: The effects of manufacturing errors on transmission characteristics are analyzed for a polymer vertical coupling microring resonator. Calculated results show that the errors cause a shift and shape change of the transmission spectrum compared to the designed case without errors. Furthermore, accumulation and compensation for the errors is researched. In order to realize the normal filtering for the fabricated microring resonator device, some allowed errors are discussed.

Key words: microring resonator; manufacturing error; polymer; transmission spectrum

DOI: 10.1088/1674-4926/33/10/104007 **PACC:** 4280L; 4282

1. Introduction

Microring resonator (MRR) devices have many applications in optical communications including wavelength filtering[1, 2], lasing[3, 4], multiplexing and demultilpexing[5, 6], modulating[7, 8], and switching[9, 10] because of their excellent features, such as low costs, compact conformation, high integrated level, low insertion loss and low crosstalk.

The excellent performance of MRR devices depends on accurate structural design and sophisticated production techniques. Fortunately, the structural design can be done by the computer. However, manufacturing errors are hard to avoid in the preparation of these devices, which can result in a shift and shape change of the transmission spectrum. Some previous papers reported on the impact of manufacturing errors on the characteristics of guided wave optical devices[11, 12]. Therefore, manufacturing error analysis is very important in the fabrication of MRR devices.

This paper is organized as follows. First, the parameter optimization is performed for a polymer vertical coupling MRR around the central wavelength of 1.55 μm. Then, the effects of manufacturing errors on the transmission spectrum are analyzed, and the accumulation and compensation of the manufacturing errors are investigated. In order to realize the normal filtering, the allowed manufacturing errors are discussed for the fabricated MRR device. Finally, some conclusions are reached for this device.

2. Parameter optimization

Figure 1 shows the diagram of a vertical coupled single MRR and the cross-sections and refractive index of the ring and channel. In MRR, the ring is placed on the top of the parallel channels, which are buried in the same cladding. R is the radius of the ring, $2L$ is the length of the left or right channel, and L is the length between the channel port and the coupling point. The ring and channel have identical core widths a and different core thicknesses b_1 and b_2, and have identical core refractive indices n_1 and different cladding refractive indices n_3 and n_2, respectively; n_2 is also the refractive index of the coupling layer between the ring and channel.

By using the coupled mode theory (CMT) and the transfer matrix technique (TMT), without considering the existence of the manufacturing errors, we obtain the optimization values of some parameters (see Table 1). The optimized process of these parameters is omitted to save space.

3. Manufacturing error analysis

For the above mentioned MRR device, due to the homogeneous medium around the buried channel, the channel is fabricated easier than the ring. Therefore, the manufacturing error analysis in this paper relates to the production process of the ring. Two kinds of errors are discussed: one is Δn_1 which changes the core refractive index from n_1 to $n_1 + \Delta n_1$, and another is Δb_1 which changes the core thickness from b_1 to $b_1 + \Delta b_1$.

3.1. Wavelength shift as a result of manufacturing errors

According to the microring resonant equation $2\pi R n_{\rm c} = m\lambda$, we can derive the expression of the shift of the central wavelength as

$$\Delta\lambda_0 = \frac{2\pi R}{m} \times \left(\frac{\partial n_{\rm c}}{\partial n_1}\Delta n_1 + \frac{\partial n_{\rm c}}{\partial b_1}\Delta b_1\right), \tag{1}$$

where $n_{\rm c}$ is the mode effective refractive index, which satisfies the following equations for the E^x_{00} mode[13].

$$\frac{2\pi n_x a}{\lambda_0} = 2\arctan\left[\left(\frac{n_1}{n_3}\right)^2 \frac{\sqrt{n_1^2 - n_3^2 - n_x^2}}{n_x}\right], \tag{2}$$

* Project supported by the Science and Technology Development of Jilin Province, China (Nos. 20110320, 201201078).
† Corresponding author. Email: zk.qin@yahoo.com.cn
Received 18 March 2012, revised manuscript received 23 April 2012

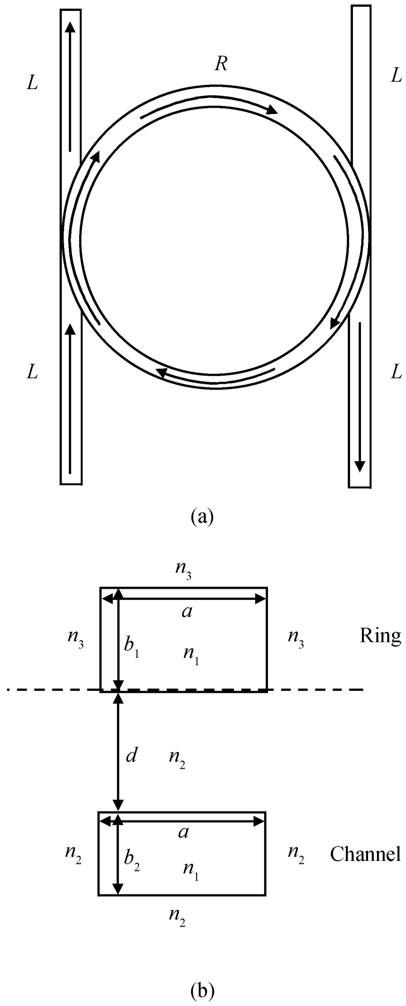

Fig. 1. (a) Diagram of a vertical coupled single MRR. (b) Cross-sections and refractive index of the ring and channel.

$$\frac{2\pi n_y b_1}{\lambda_0} = \arctan\frac{\sqrt{n_1^2 - n_2^2 - n_y^2}}{n_y} + \arctan\frac{\sqrt{n_1^2 - n_3^2 - n_y^2}}{n_y}, \tag{3}$$

$$n_c = \sqrt{n_1^2 - n_x^2 - n_y^2}. \tag{4}$$

Figure 2 presents a 3D graphic and a 2D graphic for a shift of the central wavelength $\Delta\lambda_0$ caused by the errors Δn_1 and Δb_1. It can be seen that when Δn_1, $\Delta b_1 > 0$, the wavelength shift $\Delta\lambda_0 > 0$. In contrast, when Δn_1, $\Delta b_1 < 0$, the wavelength shift $\Delta\lambda_0 < 0$. The larger the absolute values of Δn_1 and Δb_1, the larger the wavelength shift $\Delta\lambda_0$. The wavelength shift is within a range of –1.5 nm $\leqslant \Delta\lambda_0 \leqslant$ 1.5 nm, which is much less than that of the FSR, which is 17.5 nm. From Fig. 2(b) we can measure the relative errors within the ranges of $-1.54 \times 10^{-3} \leqslant \Delta n_1 \leqslant 1.54 \times 10^{-3}$ and –28.8 nm $\leqslant \Delta b_1 \leqslant$ 28.8 nm, respectively.

Table 1. Optimized values of parameters of a polymer vertical coupling MRR.

Parameter	Value
Central wavelength	$\lambda_0 = 1.55\ \mu$m
Refractive index of cores of ring and channel	$n_1 = 1.6278$
Refractive index of claddings of channel	$n_2 = 1.465$
Refractive index of air claddings of ring	$n_3 = 1$
Core width of ring and channel	$a = 2.0\ \mu$m
Core thickness of ring	$b_1 = 1.38\ \mu$m
Core thickness of channel	$b_2 = 1.0\ \mu$m
Thickness of coupling layer	$d = 0.68\ \mu$m
Resonant order	$m = 81$
Radius of ring	$R = 13.0\ \mu$m
Free spectral range	FSR = 17.5 nm
Propagation loss coefficient	$2\alpha_p = 0.5$ dB/cm
Distance	$L = 2000\ \mu$m

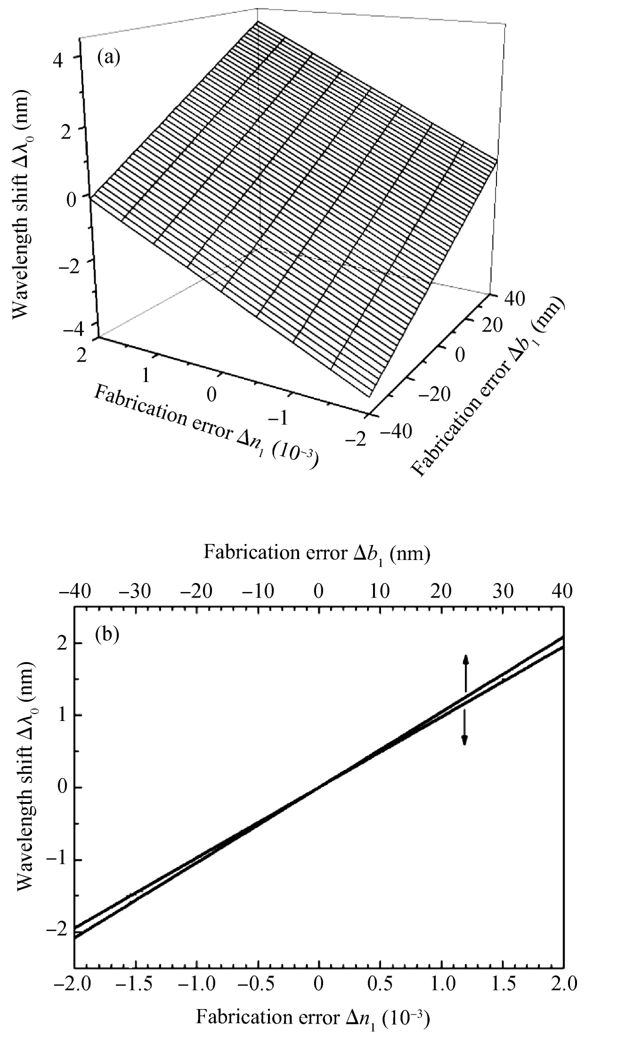

Fig. 2. (a) 3D and (b) 2D graphic for a shift of the central wavelength $\Delta\lambda_0$ caused by the errors Δn_1 and Δb_1.

3.2. Shape change of the transmission spectrum because of manufacturing errors

After the signal light is input into the channel, it couples into the ring by a coupling layer, and then resonates if it meets with the resonance conditions. By using the CMT and

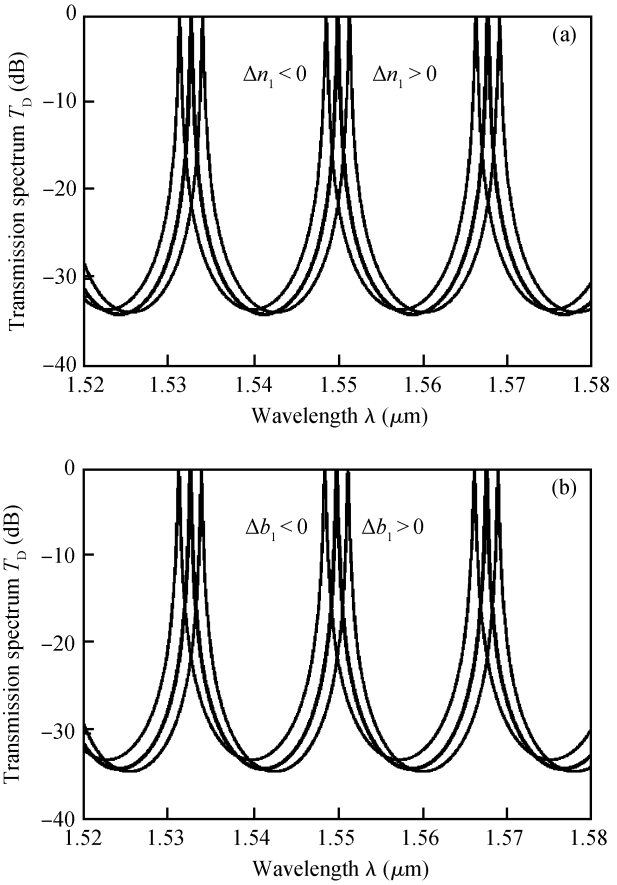

Fig. 3. Effects of the manufacturing errors (a) Δn_1 and (b) Δb_1 on the transmission spectra.

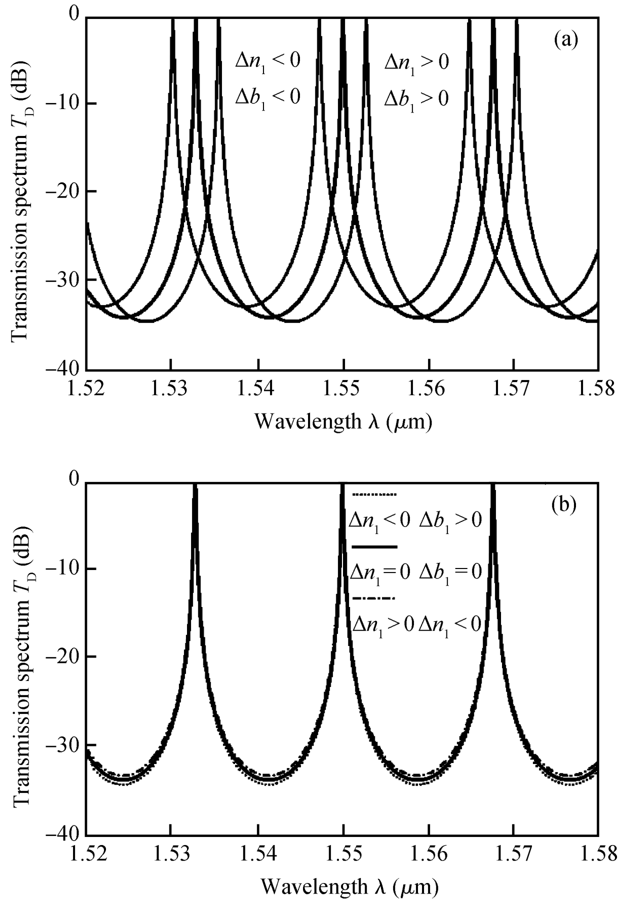

Fig. 4. Effects of the (a) accumulation and (b) compensation of manufacturing errors on the transmission spectra.

the TMT, the transfer function, i.e., the transmission spectrum, from the lower port of the left channel to the lower port of the right channel $T_\mathrm{D}(\lambda)$ can be expressed as

$$T_\mathrm{D}(\lambda)(\mathrm{dB}) = 10\lg\left|\frac{\kappa^2\exp(-\mathrm{j}\phi)}{1-(1-\kappa^2)\exp(-\mathrm{j}2\phi)}\exp(-\mathrm{j}2\psi)\right|^2, \quad (5)$$

where ϕ is the phase when the light travels an arc of πR in the microring, ψ is the phase when the light travels a distance of L in the channel. κ is the amplitude coupling ratio between the ring and the channel, which can be seen in Ref. [14].

Figure 3 shows the effects of the manufacturing errors Δn_1 and Δb_1 on the transmission spectrum. We select the following two groups of values of the manufacturing errors which produce a shift of –1.5 or 1.5 nm: (a) $\Delta b_1 = 0$, $\Delta n_1 = -1.54 \times 10^{-3}$, 1.54×10^{-3}, and (b), $\Delta n_1 = 0$, $\Delta b_1 = -28.8$ nm, 28.8 nm. For comparison, the relative curves of the theoretical design of $\Delta n_1 = \Delta b_1 = 0$ are plotted.

From Fig. 3, we can see the manufacturing errors cause the shift of the transmission spectrum. Compared with the relative errors $\Delta n_1 = 0$ and $\Delta b_1 = 0$, if the relative errors Δn_1, $\Delta b_1 > 0$, the transmission spectrum shifts to the right, on the contrary, if the relative errors Δn_1, $\Delta b_1 < 0$, the transmission spectrum shifts to the left. We can also see that the effect of Δn_1 on the minimum intensity of the nonresonant light is minor compared with that of Δb_1.

3.3. Accumulation and compensation of manufacturing errors

Figure 4 shows the effects of the accumulation and the compensation of manufacturing errors on the transmission spectra. In Fig. 4(a), we take one group of values to be $\Delta n_1 = -1.54 \times 10^{-3}$ and $\Delta b_1 = -28.8$ nm, and another to be $\Delta n_1 = 1.54 \times 10^{-3}$ and $\Delta b_1 = 28.8$ nm. In Fig. 4(b), one group of values is $\Delta n_1 = -1.54 \times 10^{-3}$ and $\Delta b_1 = 28.8$ nm, and another is $\Delta n_1 = 1.54 \times 10^{-3}$ and $\Delta b_1 = -28.8$ nm. For comparison, the relative curves of the theoretical design of $\Delta n_1 = \Delta b_1 = 0$ are also plotted.

From Fig. 4(a), we can see when the values Δn_1 and Δb_1 are both positive or both negative, i.e., Δn_1, $\Delta b_1 > 0$ or Δn_1, $\Delta b_1 < 0$, the accumulation of the manufacturing errors would appear, which increases the shift and shape change of the transmission spectrum. On the contrary, from Fig. 4(b), we can also see when one is positive and another is negative between the values Δn_1 and Δb_1, that is, when $\Delta n_1 < 0$ and $\Delta b_1 > 0$, or when $\Delta n_1 > 0$ and $\Delta b_1 < 0$, the compensation of manufacturing errors would occur, which reduces the shift and shape change of the transmission spectrum. In this case, the shift of the transmission spectrum is very close to zero, and the shape change of the transmission spectrum is very small compared to the designed case without errors.

4. Conclusion

Based on the preceding analysis and discussion of the presented MRR device, conclusions are reached as follows.

The manufacturing errors Δn_1 and Δb_1 cause the shift and shape change of the transmission spectrum. For different values of Δn_1 and Δb_1, the transmission spectrum would be obviously different. Therefore, we must control the manufacturing errors within a proper range to ensure the MRR device works with normal filtering function. If manufacturing errors are allowed within the ranges of $-1.54 \times 10^{-3} \leqslant \Delta n_1 \leqslant 1.54 \times 10^{-3}$ (when $\Delta b_1 = 0$) and $-28.8 \text{ nm} \leqslant \Delta b_1 \leqslant 28.8$ nm (when $\Delta n_1 = 0$), the shift is controlled within the range of -1.5 nm $\leqslant \Delta\lambda_0 \leqslant 1.5$ nm.

The accumulation of manufacturing errors can increase the shift and shape change of the transmission spectrum, while the compensation of the manufacturing errors can reduce the shift and shape change of the transmission spectrum. Therefore, we should avoid the accumulation and utilize the compensation of the manufacturing errors to improve the performance of the MRR device. For example, when the manufacturing errors are $\Delta n_1 = -1.54 \times 10^{-3}$ and $\Delta b_1 = 28.8$ nm, or $\Delta n_1 = 1.54 \times 10^{-3}$ and $\Delta b_1 = -28.8$ nm, the shift of the transmission spectrum is very close to zero, and the shape change of the transmission spectrum is very small compared with the theoretical design of $\Delta n_1 = \Delta b_1 = 0$.

References

[1] Zhou L J, Poon A W. Electrically reconfigurable silicon microring resonator-based filter with waveguide-coupled feedback. Opt Express, 2007, 15(15): 9194

[2] Yan Xin, Ma Chunsheng, Xu Yuanzhe, et al. Theoretical analysis of $m \times n$ microring resonator array on silicon. Chinese Journal of Semiconductors, 2005, 26(11): 2223

[3] Liu B, Shakouri A, Bowers J E. Wide tunable double ring resonator coupled lasers. IEEE Photonics Technol Lett, 2002, 14(5): 600

[4] Chu T, Fujioka N, Ishizaka M. Compact, lower-power-consumption wavelength tunable laser fabricated with silicon photonic-wire waveguide micro-ring resonators. Opt Express, 2009, 17(16): 14063

[5] Wang X Y, Ma C S, E S L, et al. Parameter optimization and characteristic analysis of a polymer microring resonant wavelength multiplexer. Opt Laser Technol, 2005, 37(4): 337

[6] Yan Xin, Ma Chunsheng, Wang Xianyin, et al. Characteristic of a vertically-coupled triple microring resonant wavelength multi/demultiplexer. Chinese Journal of Semiconductors, 2006, 27(6): 1103

[7] Tazawa H, Steier W H. Analysis of ring resonator-based traveling-wave modulators. IEEE Photonic Technol Lett, 2006, 18(1): 211

[8] Dong P, Shafiiha R, Liao S, et al. Wavelength-tunable silicon microring modulator. Opt Express, 2010, 18(11): 10941

[9] Tian Y H, Zhang L, Ji R Q, et al. Demonstration of a directed optical encoder using microring-resonator-based optical switches. Opt Lett, 2011, 36(19): 3795

[10] Tang J X, Jin Y H, Chang Z J, et al. Genetic algorithm optimization of tunable wavelength selection photonic switch using a microring resonator. Opt Eng, 2011, 50(9): 094002

[11] Qin Z K, Ma C S, Li D L, et al. Analysis for fabrication errors of arrayed waveguide grating multiplexers. Opt Laser Technol, 2008, 40(2): 235

[12] Ma C S, Yan X, Xu Y Z, et al. Analysis of a 1 × 16 polymer microring resonant wavelength demulti/multiplexer with double seriated identical microrings in every filter element. J Opt A: Pure Appl Op, 2005, 7(3): 135

[13] Marcatili E A J. Dielectric rectangular waveguide and directional coupler for integrated optics. Bell Sys Tech J, 1969, 48(7), 2071

[14] Yan X, Ma C S, Xu Y Z, et al. Characteristics of vertical bent coupling between straight and curved rectangular optical waveguides. Optik—International Journal for Light and Electron Optics, 2005, 116(8): 397